

Available at www.sciencedirect.comjournal homepage: www.elsevier.com/locate/watres

Modeling the behaviors of adsorption and biodegradation in biological activated carbon filters

Chung-Huei Liang^a, Pen-Chi Chiang^{a,*}, E-E Chang^b

^aGraduate Institute of Environmental Engineering, National Taiwan University, No. 71, Chou-shan Road, Taipei 106, Taiwan

^bDepartment of Medicine, Taipei Medical University, 250 Wu Hsing Street, Taipei 110, Taiwan

ARTICLE INFO

Article history:

Received 27 December 2006

Received in revised form

9 May 2007

Accepted 15 May 2007

Available online 21 May 2007

Keywords:

Adsorption

Biodegradation

Biological activated carbon (BAC)

Granular activated carbon (GAC)

Numerical model

ABSTRACT

This investigation developed a non-steady-state numerical model to differentiate the adsorption and biodegradation quantities of a biological activated carbon (BAC) column. The mechanisms considered in this model are adsorption, biodegradation, convection and diffusion. Simulations were performed to evaluate the effects of the major parameters, the packing media size and the superficial velocity, on the adsorption and biodegradation performances for the removal of dissolved organic carbon based on dimensionless analysis.

The model predictions are in agreement with the experimental data by adjusting the liquid-film mass transfer coefficient (k_{bf}), which has high correlation with the Stanton number. The Freundlich isotherm constant (N_F), together with the maximum specific substrate utilization rate (k_t) and the diffusion coefficient (D_t), is the most sensitive variable affecting the performance of the BAC. Decreasing the particle size results in more substrate diffusing across the biofilm, and increases the ratio of adsorption rather than biodegradation.

© 2007 Elsevier Ltd. All rights reserved.

1. Introduction

The biological activated carbon (BAC) process, which contains adsorption and biodegradation mechanisms, has been widely used in water and wastewater treatments for lowering the regeneration cost and prolonging the life of granular activated carbon (GAC) beds. Researchers and operators have been attempting to elucidate each mechanism for the purpose of simulation and optimization. For biodegradation, Hozalski et al. (1995) reported that the removal efficiency did not vary significantly under a certain empty-bed contact time (EBCT) ranging between 4 and 20 min. Melin and Ødeggard (2000) indicated that the optimum EBCT was approximately 20 min, since longer EBCT could not significantly increase the removal efficiency. Rittmann et al. (2002) reported that EBCT greater than 3.5 min had insignificant effects on dissolved

organic carbon (DOC) removal in pilot filters treating ozonated groundwater. Li et al. (2006) reported that the optimum EBCT was 15 min for an ozone-BAC process to treat raw waters.

A well-validated mathematical model can provide valuable information to assess and predict the performance of BAC, and some representative models are listed in Table 1 (Chang and Rittmann, 1987; Sakoda et al., 1996; Walker and Weatherley, 1997; Abumaizar et al., 1997; Hozalski and Bouwer, 2001; Badriyha et al., 2003). Chang and Rittmann (1987) developed a mathematical model that could quantify the extent of adsorption and biodegradation. One of its remarkable contributions is to illustrate and quantify the mass transfer of substrates diffusing through the biofilm, metabolized by microbes, and finally reaching the surface of GAC. The limitation is that it cannot be used under unsteady or plug-flow conditions. Sakoda et al. (1996) suggested a theoretical

*Corresponding author. Tel.: +886 2 2362 2510; fax: +886 2 2366 1642.

E-mail address: pcchiang@ntu.edu.tw (P.-C. Chiang).

0043-1354/\$ - see front matter © 2007 Elsevier Ltd. All rights reserved.

doi:10.1016/j.watres.2007.05.024

Nomenclature			
A_f	surface area of a BAC granule (L^2)	N_{Sh}	Sherwood number (dimensionless)
b_{tot}	total decay coefficient ($1/T$)	N_{St}	Stanton number (dimensionless)
d_p	packing media diameter (L)	q_0	Langmuir isotherm coefficients (M/M)
D_f	diffusivity in biofilm (L^2/T)	q_a	adsorption capacity (M/M)
D_z	dispersion coefficient in the liquid phase (L^2/T)	r_f	biofilm radius (L)
K_b	half-velocity concentration in water (M/L^3)	r_g	GAC granule radius (L)
k_b	max. specific substrate utilization rate in water (M/CFU-T)	S_b	substrate concentration in the liquid phase (M/L^3)
k_{bf}	liquid-film mass transfer coefficient (dimensionless)	S_{b0}	influent concentration (M/L^3)
K_f	half-velocity concentration in biofilm (M/L^3)	S_f	substrate concentration in the biofilm (M/L^3)
k_f	max. specific substrate utilization rate in biofilm (M/CFU-T)	V_g	volume of a GAC granule (L^3)
k_F	Freundlich isotherm coefficients (dimensionless)	x	distance along the BAC column (L)
K_L	Langmuir isotherm coefficients (dimensionless)	X_b	cell density in the liquid phase (CFU/ L^3)
L_c	column length (L)	X_f	biofilm density (CFU/ L^3)
L_f	length of the biofilm (L)	Y	specific yield (CFU/M)
m_g	mass of a GAC granule (M)	u_s	superficial velocity (L/T)
N_{Da}	Damköhler number (dimensionless)	Greek symbols	
N_F	Freundlich isotherm coefficients (dimensionless)	ε	porosity (dimensionless)
N_{Re}	Reynolds number (dimensionless)	ν	kinetic viscosity of the bulk solution (L^2/T)
		ρ_g	GAC granule apparent density (M/L^3)

model for a BAC column, in which the mechanisms included dispersion, convection, biodegradation and adsorption. The primary assumption for simplifying is that the substrate concentration on the interface between the biofilm and the

GAC is identical to that in the bulk solution. However, this assumption implies that there is no concentration reduction within the biofilm; thus, that model is not fit for the condition with thick biofilm. In 1997, Walker and Weatherley proposed a

Table 1 – Some of the representative BAC models

Reactor type	Mechanisms considered ^a	Kinetic condition				Mass transport description ^b	Solution method	References
		Substrate in bulk phase	Substrate in biofilm	Biofilm amount	Substrate in GAC			
Complex mixing	A, B	Non-steady monod	Monod	Non-steady	Non-equilibrium	1, 2, 3, 4, 5	Analytical	Chang and Rittmann (1987)
Column	A, B, C, D	Non-steady no biodegradation	n.a. ^c	Steady	Equilibrium	1	Analytical	Sakoda et al. (1996)
Column	A, B	Uniform Monod	Monod	Non-steady	n.a. ^c	1	Analytical	Walker and Weatherley (1997)
Column	A, B, C	Non-steady no biodegradation	Monod	Steady	Non-equilibrium	1, 5	Analytical	Abumaizar et al. (1997)
Column	B, C, D	Non-steady Monod	Monod	Non-steady	n.a. ^c	1, 2, 3	Numerical	Hozalski and Bouwer (2001)
Column	A, B, C, D	Non-steady no biodegradation	Monod	Non-steady	Non-equilibrium	1, 2, 3, 4, 5	Numerical	Badriyha et al. (2003)

^a A = adsorption, B = biodegradation, C = convection, D = dispersion.

^b 1 = bulk phase, 2 = interface between bulk phase and biofilm, 3 = biofilm, 4 = interface between biofilm and GAC, 5 = GAC.

^c Not analyzed in the article.

simplified predictive model for BAC fixed beds based on Monod kinetics. Their mathematical development is under the assumptions that the BAC system is a simple combination of adsorption and biodegradation, so that the model can be executed without the detailed analysis of diffusion and biodegradation in the biofilm. A detailed biofilter model was reported by Hozalski and Bouwer in 2001. In their model, the length of the biofilm is controlled by biotic processes as well as mass transfer dynamically. In 2003, Badriyha et al. proposed a mathematical model for the design and the performance prediction of a bioadsorber reactor. Their governing equations contain the terms of adsorption, biodegradation, convection and dispersion. Although it is able to solve the non-steady-state condition, the mass flux entering the biofilm from bulk solution will be restricted after the adsorption capacity is exhausted since the substrate concentrations are assumed to be identical on the both sides of the adsorbent–biofilm interface.

This research developed a numerical model to simulate both adsorption and biodegradation quantities of a BAC column under a non-steady-state condition, so as to predict the effluent concentration, biomass profiles and the residual capacity of adsorption. The basic assumptions of our model are that (1) the granules used in BAC are spherical in shape, and the biofilm is homogeneous and the density of the biofilm is constant; (2) the biodegradation reactions can be neglected in the pores of the granules, because the size of most meso- or micro-pores (<0.05 μm) of GAC are less than the size of a microbe; (3) desorption after the saturation of the GAC is not taken into consideration because this model focuses on the simulation of virgin GAC; (4) a peeled-off biofilm is neglected as the source of DOC; (5) there is no competition or inhibition between two substrates. We also performed a series of bench-scale continuous column tests for model calibration and validation, and assessed the effects of packing media size on adsorption and biodegradation performances with the dimensionless analysis.

2. Materials and method

2.1. Model development

The governing equation is based on mass balance for the substrate concentration in the liquid phase of the BAC column:

$$\begin{aligned} \varepsilon \frac{\partial S_{b,i}}{\partial t} = & D_{z,i} \frac{\partial^2 S_{b,i}}{\partial x^2} - v_s \frac{\partial S_{b,i}}{\partial x} - \frac{(1-\varepsilon)}{V_g} \\ & \times \int_0^{L_f} \frac{k_{f,i} X_f S_{f,i}}{K_{f,i} + S_{f,i}} 4\pi(r_f + r_g)^2 dr_f \\ & - (1-\varepsilon)\rho_g \frac{\partial q_{a,i}}{\partial t} - \varepsilon \left(\frac{k_{b,i} X_b S_{b,i}}{K_{b,i} + S_{b,i}} \right), \end{aligned} \quad (1)$$

where ε is the bed porosity of the BAC column; $S_{b,i}$ is the substrate concentration in the liquid phase (M/L), and $i = 1, 2$ denotes components 1 and 2, respectively; $D_{z,i}$ is the dispersion coefficient in the liquid phase (L²/T), x is the distance along the BAC column (L), v_s is the superficial velocity (L/T); V_g is the volume of a GAC granule (L³); L_f is the length of the biofilm (L); $k_{f,i}$ is the maximum utilization rate in the biofilm

(M/T-cell); X_f is the cell density of the biofilm (cell/L³); $S_{f,i}$ is the substrate concentration in the biofilm (M/L³); $K_{f,i}$ is the Monod half-velocity coefficient in the biofilm (M/L³); r_f and r_g are the radius of the biofilm and the GAC granule, respectively (L); ρ_g is the GAC granule density (M/L³); $q_{a,i}$ is the adsorption capacity (M/M); $k_{b,i}$ is the maximum utilization rate in the liquid phase (M/T-cell); X_b is the cell density in the liquid phase (cell/L³); and $K_{b,i}$ is the Monod half-velocity coefficient in the liquid phase (M/L³).

The boundary conditions (BC) of the dispersion–advection reaction equation are

$$\text{BC 1: } S_{b,i} = S_{b0,i} \quad x = 0, \quad t \geq 0, \quad (2)$$

$$\text{BC 2: } \left. \frac{\partial S_{b,i}}{\partial x} \right|_{x=L_c} = 0, \quad (3)$$

where L_c is the length of the BAC column (L).

The pathways of substrates after entering the biofilm are biodegradation and metabolism-independent processes such as biosorption (Aksu and Tunç, 2005). The non-steady-state form of mass transfer and biodegradation reaction within biofilms, based on Fick's law and Monod equation, can be expressed as

$$\frac{\partial S_{f,i}}{\partial t} = D_{f,i} \frac{\partial^2 S_{f,i}}{\partial r_f^2} - \frac{k_{f,i} S_{f,i}}{K_{s,i} + S_{f,i}} X_f \quad 0 \leq r_f \leq L_f, \quad (4)$$

where $D_{f,i}$ is the diffusivity within the biofilm (L²/T). Eq. (4) describes a non-steady-state biofilm condition, where diffusion and reaction are simultaneously occurring. One BC for Eq. (4) is that a diffusion layer exists between the bulk solution and the biofilm, and the BC can be simplified as

$$S_{f,i}|_{r_f=0} = k_{bf,i} S_{b,i}, \quad (5)$$

where k_{bf} is a factor to estimate the concentration reduction within the diffusion layer.

Another BC for Eq. (4) describes the interface between the biofilm and the GAC surface based on the equilibrium of the substrate. In the study conducted by Chang and Rittmann (1987), they assumed that there existed an interface between the activated carbon and the biofilm, and used the Freundlich isotherm to describe the equilibrium at the interface. In this study, the Freundlich isotherm is also used to calculate the boundary concentration of the biofilm near the GAC side, which can be derived from the solid-phase concentration of the adsorbates. But for bi-component adsorbate cases, the Langmuir isotherm is used:

$$q_{a,i} = \frac{q_0 K_{L,i} C_{a,i}}{1 + K_{L,i} \sum C_{a,j}}, \quad j = 1, 2, \quad (6)$$

where q_0 is the unit-layer adsorption capacity (M/M); $K_{L,i}$ is Langmuir coefficient (L³/M); and $C_{a,i}$ is the substrate concentration on the boundary of the biofilm (M/L³).

The calculation for the adsorption capacity is based on the fact that the substrate coming out from the biofilm is identical to that absorbed by a GAC:

$$4\pi r_g^2 D_{f,i} \left. \frac{\partial S_{f,i}}{\partial r_f} \right|_{r_f=L_f} = \frac{\partial q_{a,i}}{\partial t} m_g, \quad (7)$$

where m_g is the mass of a GAC granule (M).

The substrate diffusing into biofilm will be utilized by microbes for metabolism. In a control volume, the average

biodegradation rate can be derived by integrating the Monod reaction expression and the amount of biofilm volume:

$$\left[\int_0^{L_f} \frac{k_f S_f}{K_f + S_f} X_f 4\pi(r_g + r_f)^2 dr_f \right] N_g, \quad 0 \leq r_f \leq L_f, \quad (8)$$

$$N_g = \frac{\Delta V(1 - \varepsilon)}{V_g}, \quad (9)$$

where ΔV is a control volume unit of the BAC bed (L^3) and N_g is the number of BAC granules in a control volume.

Concerning the thickness of biofilm, the major enhancing factor is the reproduction of microbes, and the shrinking factors are the shear of water and the self-decay. Hence, biofilm thickness can be described as

$$\frac{\partial L_f}{\partial t} = \frac{Y \int_0^{L_f} ((k_i S_{f,i}) / (K_{s,i} + S_{f,i}) X_f) 4\pi(r_g + r_f)^2 dr_f}{A_f X_f} - b_{tot} L_f, \quad 0 \leq r_f \leq L_f, \quad (10)$$

where Y is true yield coefficient of biomass (CFU/M); A_f is the surface area of a BAC granule (L^2); and b_{tot} is the overall loss rate of bacteria due to both decay and fluid shear (T^{-1}).

In this research, the governing equation of the bacterial density in bulk solution can be simplified as an advection-reaction form, because dispersion and the effects of growth and decay are insignificant in a macroscope (Hozalski and Bouwer, 2001):

$$\frac{\partial X_b}{\partial t} = -v \frac{\partial X_b}{\partial x} + \frac{Y k_{b,i} S_{b,i} X_b}{K_{b,i} + S_{b,i}}. \quad (11)$$

The BCs of Eq. (11) are shown below:

$$\text{BC 1: } X_b = X_0, \quad x = 0, \quad t \geq 0, \quad (12)$$

$$\text{BC 2: } \left. \frac{\partial X_b}{\partial x} \right|_{x=L_c} = 0. \quad (13)$$

2.2. Numerical solution

The governing equation of the substrate concentration in bulk solution is a second-order partial differential equation, and can be numerically approximated by the Crank–Nicolson finite difference method, with the Crout factorization method solving a tridiagonal linear system. The initial condition is

$$S_b(x, t) = 0, \quad t = 0, \quad (14)$$

$$q_a(t) = 0, \quad t = 0. \quad (15)$$

The non-steady-state substrate concentration within the biofilm is also numerically approximated by the Crank–Nicolson finite difference method, and the initial condition is

$$S_f(r_f, t) = 0, \quad t = 0. \quad (16)$$

The program was written in FORTRAN 90 developed by Microsoft PowerStation.

2.3. Data analysis

The input parameters of this model were derived from our previous studies (Liang et al., 2003, 2004) and other researchers' work (Badriyha et al., 2003), listed in Table 2. In Scenario I, the target compound is an ozonation by-product, represented

as glyoxalic acid, which denotes a highly biodegradable but low absorbable substrate (Liang et al., 2003). In Scenario II, the target compounds are *p*-hydroxybenzoic acid and its ozonation intermediates, which represent the mixing of low biodegradable but highly absorbable (*p*-hydroxybenzoic acid) with highly biodegradable but low absorbable (ozonation intermediates) substrates (Liang et al., 2004). In scenario III, a pesticide alachlor is used as the target compound with acetate to support the growth of microbes (Badriyha et al., 2003).

Dimensionless parameters are calculated to determine the dynamics of the BAC reactor. In this study, the suggested dimensionless groups are

$$\text{Reynolds number} = N_{Re} = \frac{d_p v_s}{\nu}, \quad (17)$$

$$\text{Stanton number} = N_{St} = \frac{k_{fc} L_c}{v_s r_g}, \quad (18)$$

$$\text{Sherwood number} = N_{Sh} = \frac{k_{fc} r_g}{D_f}, \quad (19)$$

$$\text{Damköhler number} = N_{Da} = \frac{(X_f k_f / K_f) r_g^2}{D_f}, \quad (20)$$

where ν is the kinetic viscosity of the bulk solution (L^2/T); d_p is the diameter of the packing media (L); k_{fc} is the liquid film mass transfer coefficient in the column (L/T), and can be estimated by the dimensionless groups of Reynolds, Sherwood and Schmidt numbers (Wakao and Funazkri, 1978):

$$N_{Sh} = 2 + 1.1 \times N_{Re}^{1/2} N_{Sc}^{1/3}. \quad (21)$$

The Reynolds number represents the ratio between inertial force and viscous force; the Stanton number represents the ratio between liquid-film transfer and bulk transfer; the Sherwood number represents the ratio between liquid-film transfer and biofilm diffusive transfer; the Damköhler number denotes the ratio between biodegradation rate and biofilm diffusive transport. A high Damköhler number indicates that the biodegradation rate exceeds the mass transfer rate within the biofilm, which implies that less substrate can transfer to the boundary of the GAC. It should be mentioned that these dimensionless groups are developed for scaling the reactor, and different reactors can be compared by each other through these dimensionless groups. In addition, certain operational parameters, such as the particle size of packing media and the superficial velocity of the influent, reasonably dominate the performance of a BAC column. Hence, we simulate the effects of the particle size on adsorption and biodegradation, and also attempt to formulate them according to dimensional groups.

3. Results and discussion

3.1. Model calibration

This model assumes that a diffusion layer exists between the bulk solution and the biofilm; thus, we introduce a liquid-film mass transfer coefficient ($k_{b,i}$) to estimate the concentration reduction within the diffusion layer for calibrating and fitting

Table 2 – Operation conditions and parameters used for model simulation

Parameter (symbol, unit)	Scenario I (Liang et al., 2004)	Scenario II (Liang et al., 2003)	Scenario III (Badriyha et al., 2003)
BAC filter and operation specifications			
Target compound	Glyoxalic acid	p-hydroxy-benzoic acid ^a	Alachlor
Column length (L_c , cm)	50	25	5 ^b
Column diameter (d_c , cm)	5	5	1.25
Porosity (ϵ)	0.4	0.4	0.4 ^b
Superficial velocity (v_s , cm/h)	300	1200	972
GAC granule radius (r_g , cm)	0.11	0.11	0.018
GAC granule apparent density (ρ_g , g/cm ³)	0.88	0.88	1.25
Temperature (°C)	25	25	25
Flow type	Downflow	Downflow	Upflow
Recycle ratio	0	0	5
Substrate properties			
Influent concentration (S_{b0} , mg/L)	0.4 (as DOC)	2.5 and 0.6 (as DOC)	0.8 (as alachlor)
Dispersion coefficient (D_z , cm ² /h)	297	1296	154
Diffusivity in biofilm (D_f , cm ² /h)	2.9×10^{-2}	2.3×10^{-2}	1.3×10^{-2}
Biokinetic and bioassay constants			
Max. specific substrate utilization rate in water, biofilm (k_b and k_f , mg/CFU-h)	1.7×10^{-10}	2.1×10^{-11}	0.66 ^c
Half-velocity concentration in water, biofilm (K_b and K_f , mg/L)	0.1	10	60
Specific yield (Y , CFU/mg)	6.45×10^8	6.45×10^8	0.6 ^c
Biofilm density (X_f , CFU/L)	5.0×10^{13}	5.0×10^{13}	35 (mg/cm ³)
Total decay coefficient (b_{tot} , 1/day)	0.25	0.25	0.072
Adsorption constants			
Freundlich isotherm coefficients (k_f , N_f)	14.1, 8.3	21.0, 3.7	102, 3.2
Langmuir isotherm coefficients (q_0 , K_i)	18.9, 9.1	25.1, 11.1	102, 0.31

^a With its ozonation intermediates; the properties of the intermediates set as Scenario I.

^b Assumption.

^c Based on (mg-substrate/mg-biomass) or (mg-biomass/mg-substrate).

the experimental data. The best k_{bf} value for simulation was acquired by adjusting the output to the experimental data (Liang et al., 2004), and the results were represented quantitatively by the least-square value

$$\text{Least-square value} = \frac{1}{N} \sum_{\text{all data points}} \sqrt{\frac{(C_{\text{eff}}^{\text{sim}} - C_{\text{eff}}^{\text{exp}})^2}{(C_{\text{eff}}^{\text{exp}})^2}} \quad (22)$$

The average least-square value provides a quantitative comparison of the agreement between the simulation and the experimental data. As the average least-square value increases, the level of agreement between the two simulations decreases. Meanwhile, a higher k_{bf} permits a higher driving force on the biofilm boundary, and makes the substrate concentration profile higher within the biofilm; as a consequence, the amounts of both biodegradation and adsorption increase at the same time.

Fig. 1 illustrates the correlation between the liquid-film mass transfer coefficient (k_{bf}) and the Stanton number (N_{St}). The Stanton number represents the ratio of the liquid-film transfer to the bulk transfer, and has inverse proportion to the particle size and the superficial velocity; that is, larger particle sizes or higher superficial velocities lead to a low liquid-film

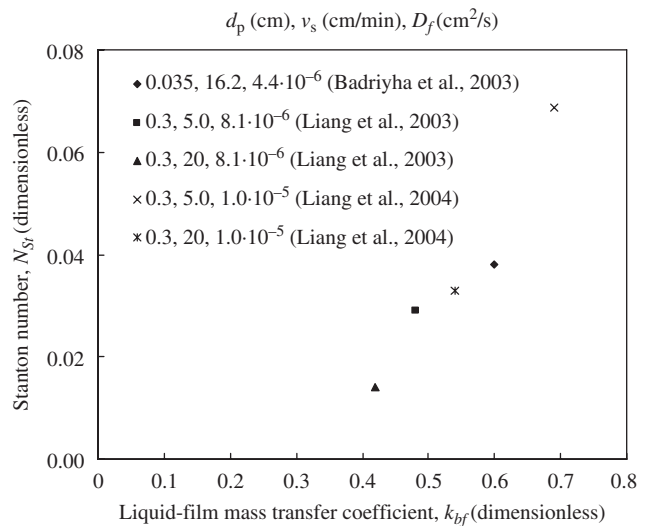


Fig. 1 – Correlation between the liquid-film mass transfer coefficient (k_{bf}) and the Stanton number (N_{St}).

mass transfer. Escudié et al. (2005) indicated that the efficiency of the biological reactions was limited by the substrate transfer onto the biofilm. From Fig. 1, it is observed

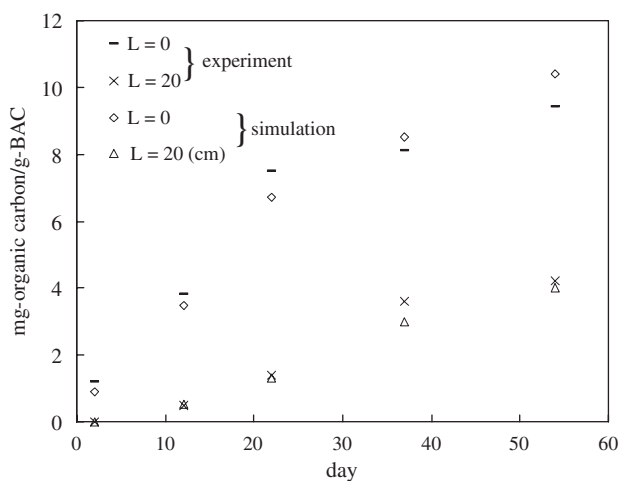
that the liquid-film mass transfer coefficient correlates with the Stanton number; that is, increasing the Stanton number can enhance the mass transfer from bulk solution into the biofilm.

3.2. Model verification

Fig. 2 illustrates the adsorption capacities of the BAC granules according to our previous study (Scenario I) as well as the simulation results, which provide a criterion whether the model fits the experimental data. In Fig. 2, acceptable errors exist between the model prediction and the experimental data; nonetheless, it implies that this model is a reasonable instrument for simulating the adsorption behavior of the BAC column.

Remarkable evidence is that the adsorbed DOC on BAC granules is less than that on GAC. During the simulation processes, the liquid-phase substrate concentration in the BAC column was lower than that in the GAC column because of the biological degradation; consequently, the equilibrium concentration of the BAC granules was lower than that of the GAC granules in the solid phase. In other words, the biodegradation mechanism can efficiently reduce the organic loading of the BAC granules.

To differentiate the quantities of adsorption and biodegradation separately, Fig. 3a and b shows the cumulative removal of *p*-hydroxybenzoic acid and the ozonation intermediates by the two mechanisms. Using the parameters of Scenario II, the simulation results are in accordance with the experimental data. As expected, the major mechanism for the removal of *p*-hydroxybenzoic acid is adsorption, and of the ozonation intermediates is biodegradation. The results of both experiment and simulation lead to a consensus that the BAC column cannot effectively remove the substrate until biodegradation reaches the point of equilibrium. In this research,



Dimensionless group
 $N_{Re} = 20.6$ $N_{Sh} = 48.5$
 $N_{Sc} = 864$ $N_{St} = 3.3 \cdot 10^{-2}$
 $N_{Da} = 8.6 \cdot 10^4$

Fig. 2 – Organic carbon adsorbed on the GAC granules under various depths.

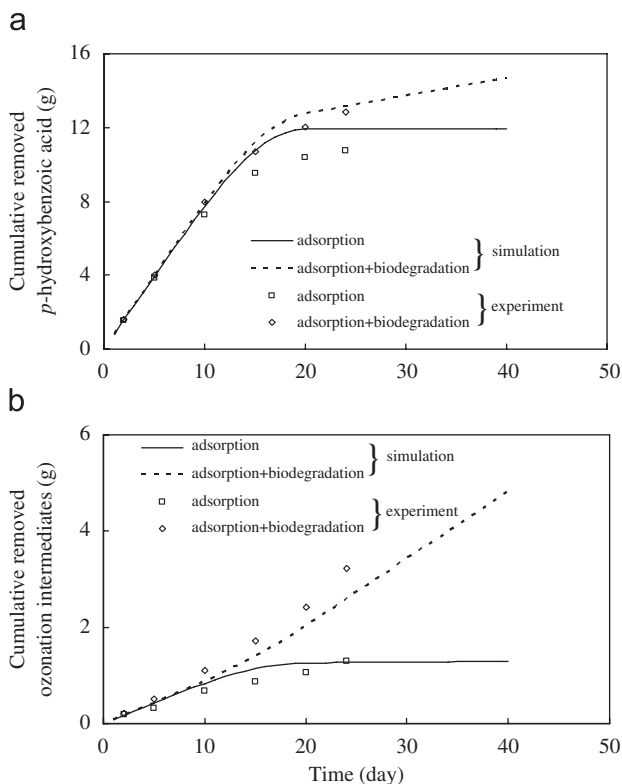


Fig. 3 – Cumulative removal of DOC by adsorption and biodegradation: (a) *p*-hydroxybenzoic acid and (b) ozonation intermediates.

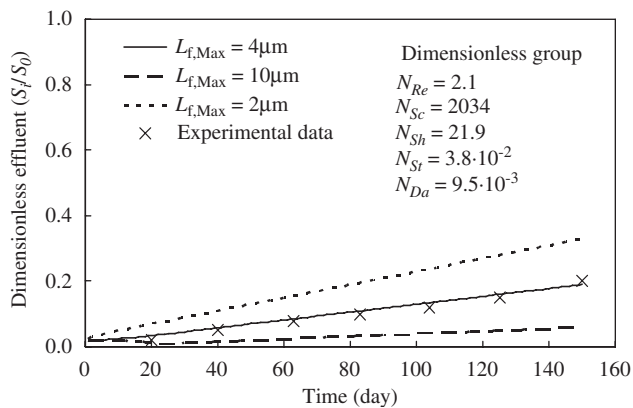


Fig. 4 – Simulation for the removal of alachlor (Badriyha et al., 2003).

biodegradation changed from an unsteady to a steady state after approximately 2–3 weeks of operation when the effluent concentrations varied within a narrow range.

In addition, Fig. 4 denotes that our model is also validated well by other researchers' results (Badriyha et al., 2003). In their experimental system, some facts should be noted. First, they recycled the effluent back to the influent (recycle ratio = 5), so that the influent concentration was amplified if the target compound existed in the effluent. Second, they added acetate in the feed solution to sustain the growth of microbes; that is, the behavior of biodegradation was

controlled by acetate as well asalachlor. Even though acetate did not influence the behavior of adsorption, it should be taken into consideration for biodegradation. The Stanton number and the Sherwood number of their experimental system are of the same order as our experimental system, but their Schmidt number is greater, which implies that viscous force has more influences on their system. The remarkable difference between the two systems is the Damköhler number; our Damköhler number is about seven orders (Scenario I) and four orders (Scenario II) higher than theirs, respectively. This is because they used a much finer GAC (0.035 cm in diameter) and the target compoundalachlor is less biodegradable (0.011 min^{-1}). As a result, the limiting factor is the biodegradation rate rather than the biofilm mass transfer in their system.

3.3. Sensitivity analysis

The sensitivity analysis, which quantifies the magnitude of each variable affecting the simulation results, was executed by using the least-squares analysis to acquire quantitative comparisons between the baseline value and the output by increasing/decreasing the parameter. The baseline is the effluent concentration of Scenario I; meanwhile, the value of each parameter is increased 100% from its baseline value for one simulation and also decreased 50% from its baseline value for another simulation, and the results are listed in Table 3. If the adjustment of an input parameter considerably increases the least-squares value, the model is sensitive to that parameter.

The Freundlich isotherm exponential term N_F is one of the most sensitive variables as indicated by the average least-squares value between the effluent substrate curves as shown in Fig. 5a. The result is obvious because N_F determines the scale of adsorption exponentially, and results in a very large change in the simulated curve. Another remarkably sensitive variable is the maximum specific substrate utilization rate from Monod kinetics, since biodegradation is one of the key mechanisms of the BAC (Fig. 5b).

In the simulation process, the pathway of the substrates is to cross the biofilm and subsequently to be adsorbed by the activated carbon; this assumption leads to a result that the biofilm covering the BAC granules can be regarded as a resistance to the mass transfer of adsorption. As a conse-

quence, both the thickness and the diffusivity within the biofilm (D_f) determine the scale of the substrate mass flux from bulk liquid transferring to the surface of the adsorbent. D_f can, moreover, influence the concentration profile within

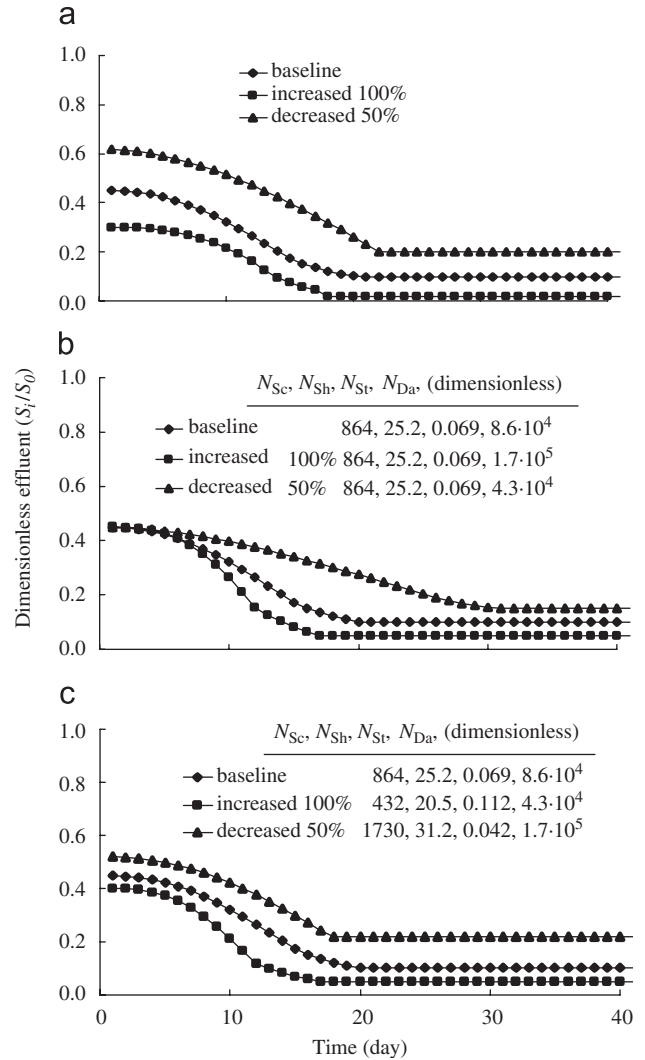


Fig. 5 – Sensitivity analysis for the input parameters: (a) Freundlich constant, N_F ; (b) maximum specific utilization rate, k_f and (c) diffusivity in biofilm, D_f .

Table 3 – The sensitivity analysis of the model input parameters

Parameter	Increased 100%	Average least-squares value	Decreased 50%	Average least-squares value
N_F (8.3)	16.6	0.57	4.2	0.91
D_f (2.9×10^{-2})	5.8×10^{-2}	0.41	1.5×10^{-2}	0.71
k_f (1.7×10^{-10})	3.4×10^{-10}	0.35	0.9×10^{-10}	0.71
k_F (14.1)	28.2	0.13	7.1	0.45
b_{tot} (0.25)	0.5	0.34	0.13	0.17
K_f (0.1)	0.2	0.30	0.05	0.16
Y (6.45×10^8)	1.28×10^9	0.08	3.2×10^8	0.54
X_f (5.0×10^{13})	1.0×10^{14}	0.13	2.5×10^{13}	0.14

the biofilm, and consequently change the magnitude of the amount of biodegradation. In this model, shifting the value of D_f dramatically changes the simulation output (Fig. 5c). In conclusion, the mass transfer within the biofilm also performs as an essential factor affecting the performance of BAC through both adsorption and biodegradation.

The simulation output is moderately sensitive to changes in the total decay coefficient (b_{tot}) and the Monod half-velocity constant (K_f). The moderate impact of K_f is due to the relatively low baseline value of the parameter of 0.1 mg/L relative to the initial substrate concentration of 0.4 mg/L. According to Monod kinetics, the influence of K_f on the overall substrate degradation rate diminishes as the value of K_f becomes insignificant relative to the range of substrate concentrations. As a result, the degradation reaction rate approaches zero order with respect to the substrate concentration.

Although the profile of active biomass is a significant property of the biofilm, this model output is relatively insensitive to the microbial density of the biofilm (X_f) and the specific yield (Y). Generally, the biofilm is composed of

extracellular polymeric substances, inert biomass and active biomass, but only the last one can provide the capacity of biodegradation. Zhang and Bishop (1994) indicated that on the outer surface the viable biomass constituted nearly all the biofilm, while near the bottom the viable part was approximately 30% of the total biomass. Another experimental study showed that the deep portion of the biofilm had a lower live-cell ratio compared with the outer surface (Ohashi et al., 1999). From the result of one-dimensional and multi-species model simulation, it was concluded that active heterotrophic bacteria dominated near the outer surface of the biofilm, while inert biomass dominated near the attachment surface (Rittmann et al., 2002). In addition, the substrate-loading rate can also affect the microstructure of biofilms. Wijeyekoon et al. (2004) showed that increasing substrate concentrations produced more compact biofilms with lower porosity, and slowly growing biofilms having porous structures were found to have higher specific activities. According to the assumption of this model, the biofilm is homogeneous both in its structure and in its density because most of the biodegradation parameters were derived from macroscale experiments.

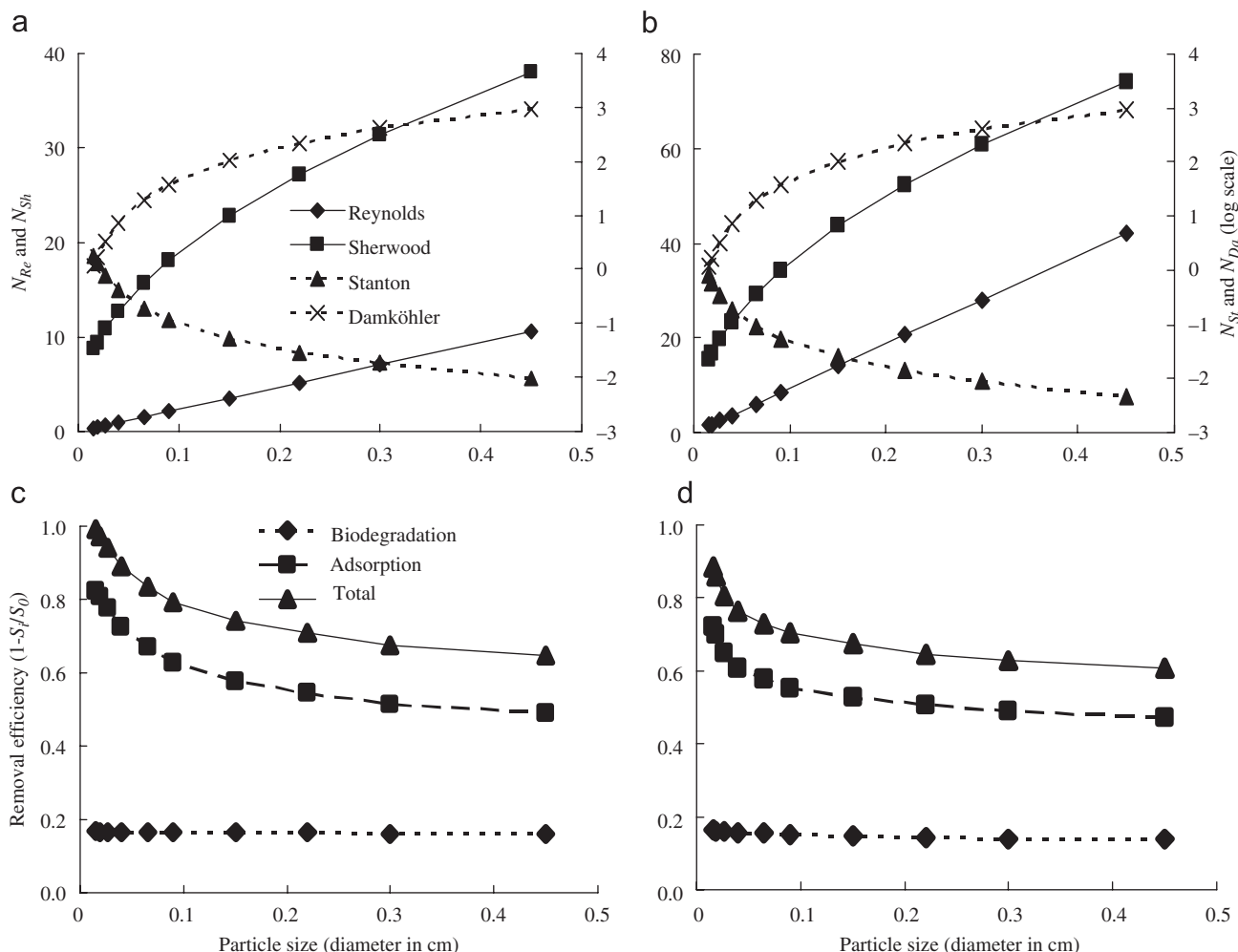


Fig. 6 – Simulations of various particle diameters for the removal of *p*-hydroxybenzoic acid. (a) and (c) Dimensionless groups and removal efficiency, $v_s = 5$ cm/min; (b) and (d) dimensionless groups and removal efficiency, $v_s = 20$ cm/min.

Nonetheless, such simplification is acceptable since this model is not very sensitive to the biofilm density, and the baseline value can tolerate a relatively uncertain range compared with the other parameters. Thus, the results of sensitivity analysis offer valuable information to operators to select the most significant parameters that determine the performance of the BAC.

3.4. Simulations for the removal efficiency of various particle sizes

To determine effects of particle size of the packing media on the removal efficiencies, a simulation procedure was computed to calculate the removal efficiency of adsorption and biodegradation of the BAC column. Apparently, decreasing the particle size results in raising the efficiency of mass transfer as well as in enhancing the removal efficiencies of both adsorption and biodegradation. The case of Scenario II with EBCT = 5 and 1.25 min ($v_s = 5$ and 20 cm/min, respectively) was performed to assess the removal efficiency of *p*-hydroxybenzoic acid operated at various particle sizes.

Fig. 6a and c shows the changes of dimensionless parameters. It is obvious that Reynolds, Sherwood and Damköhler numbers increase as the particle size increases; at the same time, Stanton number decreases. As mentioned previously, a higher Stanton number represents a higher driving force for the mass transfer from bulk solution to biofilm. This phenomenon implies that the mass transfer within the biofilm is the limiting factor when the particle size increases.

Fig. 6b and d shows the simulated removal efficiencies of adsorption and biodegradation after biodegradation equilibrium. It is evident that decreasing particle size can improve the overall removal efficiency, especially for adsorption rather than for biodegradation. According to the definition of Damköhler number, a lower Damköhler number means a lower biodegradation rate or a higher transfer rate within the biofilm, which permits more substrate to cross the biofilm toward the adsorbent. As a consequence, the adsorption ratio rises as the particle size decreases. In addition, a higher superficial velocity reflects higher Reynolds and Sherwood numbers, but a lesser Stanton number on the contrary. Hence, the overall removal efficiency decreases as the superficial increases.

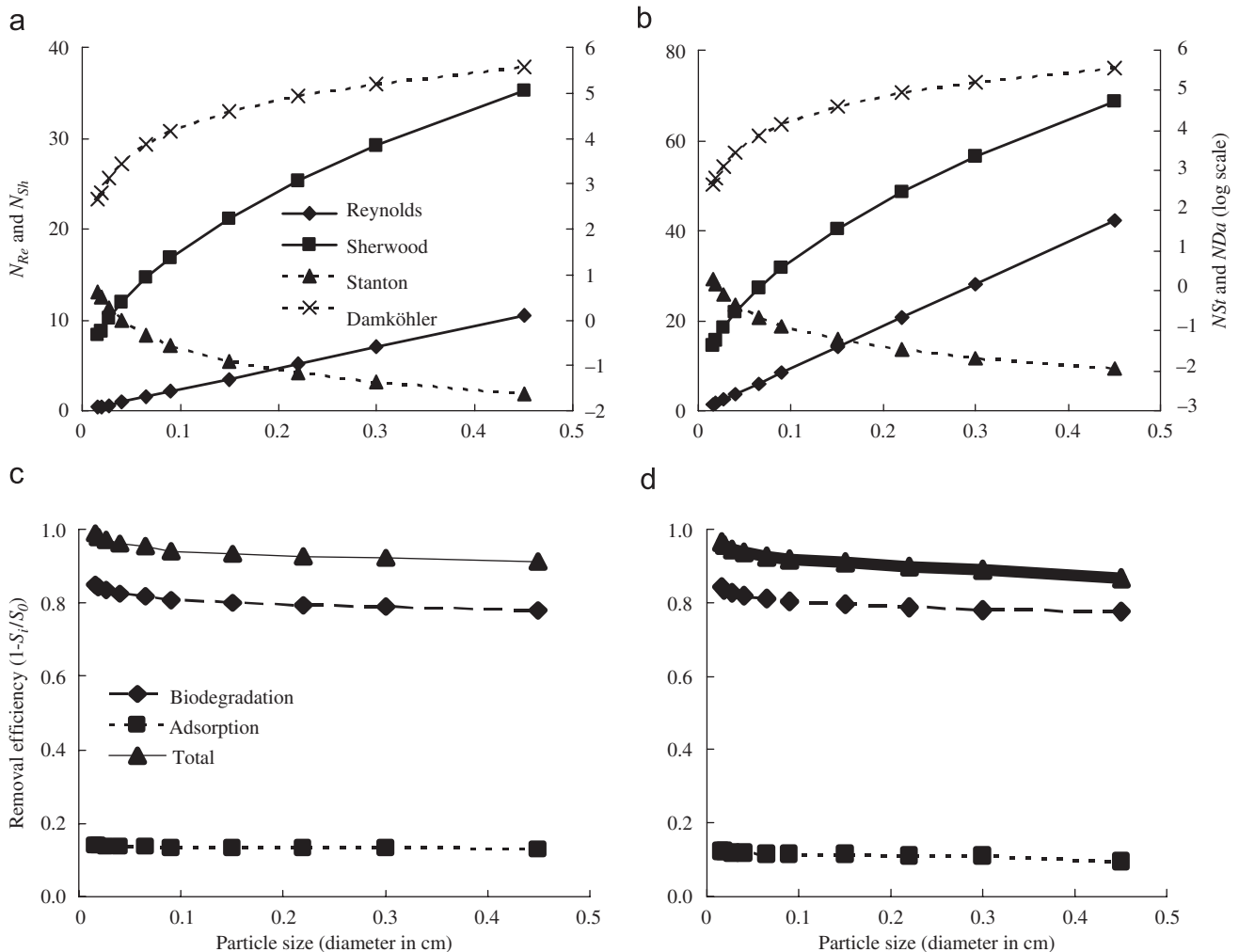


Fig. 7 – Simulations of various particle diameters for the removal of ozonation intermediates. (a) and (c) Dimensionless groups and removal efficiency, $v_s = 5$ cm/min; (b) and (d) dimensionless groups and removal efficiency, $v_s = 20$ cm/min.

The same procedure was conducted to determine effects of particle size of the packing media on the removal efficiencies of the ozonation intermediates of *p*-hydroxybenzoic acid, and the changes of dimensionless parameters are shown in Fig. 7a and c. It is also evident that Reynolds, Sherwood and Stanton numbers are the same as the simulation of *p*-hydroxybenzoic acid, but the only exception is the Damköhler number. In this case, the target compound is highly biodegradable but low absorbable, so that the Damköhler number in this case is greater than that in the *p*-hydroxybenzoic acid case.

According to the simulation above, Fig. 7b and d shows the simulated removal efficiencies of adsorption and biodegradation after biodegradation equilibrium. Decreasing particle size slightly improves the adsorption removal efficiency, and thus slightly increases the overall performance. Since the intrinsic property of ozonation intermediates is highly biodegradable but low absorbable, the magnitude of the improvement is limited.

4. Conclusions

This model provides a good approximation of the experimental data by adjusting the liquid-film mass transfer coefficients. A higher k_{bf} reflects a higher driving force on the biofilm boundary, and results in a higher substrate concentration profile within the biofilm. Furthermore, the liquid-film mass transfer coefficient has a certain correlation to the Stanton number; that is, increasing Stanton number can improve the mass transfer from bulk solution into the biofilm.

The Freundlich isotherm exponential term N_F and the maximum specific substrate utilization rate from Monod kinetics are two of the most sensitive variables. The mass transfer within the biofilm is another essential factor influencing the performance of BAC. Because D_f can shift the concentration profile within the biofilm as well as the boundary concentration for adsorption, it thus dominates the magnitude of both adsorption and biodegradation. The model output is relatively insensitive to the microbial density of the biofilm and to the specific yield; that is, the baseline value can tolerate a relatively uncertain range compared to the other parameters.

Reynolds number, together with Sherwood and Damköhler numbers, increases as the particle size increases, and results in the mass transfer within the biofilm being the limiting factor of the performance of a BAC column. On the contrary, decreasing the particle size, the condition of lower Damköhler number, leads to a lower biodegradation rate or a higher transfer rate within the biofilm. Therefore, more substrate diffuses across the biofilm, which increases the ratio of adsorption rather than biodegradation.

REFERENCES

- Abumaizar, R.J., Smith, E.H., Kocher, W., 1997. Analytical model of dual-media biofilter for removal of organic air pollutants. *J. Environ. Eng. ASCE* 123 (6), 606–614.
- Aksu, Z., Tunç, Ö., 2005. Application of biosorption for penicillin G removal: comparison with activated carbon. *Process. Biochem.* 40 (2), 831–847.
- Badriyha, B.N., Ravindran, V., Den, W., Pirbazari, M., 2003. Bioadsorber efficiency, design, and performance forecasting for alachlor removal. *Water Res.* 37 (17), 4051–4072.
- Chang, H.T., Rittmann, B.E., 1987. Mathematical modeling of biofilm on activated carbon. *Environ. Sci. Technol.* 21 (3), 273–280.
- Escudíe, R., Conte, T., Steyer, J.P., Delgenès, J.P., 2005. Hydrodynamic and biokinetic models of an anaerobic fix-bed reactor. *Process. Biochem.* 40 (7), 2311–2323.
- Hozalski, R.M., Bouwer, E.J., 2001. Non-steady state simulation of BOM removal in drinking water biofilters: model development. *Water Res.* 35 (1), 198–210.
- Hozalski, R.M., Goel, S., Bouwer, E.J., 1995. TOC removal in biological filters. *J. Am. Water Works Assoc.* 87 (12), 40–54.
- Li, L., Zhu, W., Zhang, P., Zhang, Q., Zhang, Z., 2006. AC/O₃-BAC processes for removing refractory and hazardous pollutants in raw water. *J. Hazard. Mater.* 135 (1–3), 129–133.
- Liang, C.H., Chiang, P.C., Chang, E.E., 2003. Systematic approach to quantify adsorption and biodegradation in biological activated carbon. *Ozone Sci. Eng.* 25 (5), 351–361.
- Liang, C.H., Chiang, P.C., Chang, E.E., 2004. Quantitative elucidation of the effect of EBCT on adsorption and biodegradation of biological activated carbon filters. *J. Chin. Inst. Chem. Eng.* 35 (2), 1–9.
- Melin, E.S., Ødegaard, H., 2000. The effect of biofilter rate on the removal of organic ozonation by-product. *Water Res.* 34 (18), 4464–4476.
- Ohashi, A., Koyama, T., Syutsubo, K., Harada, H., 1999. A novel method for evaluation of biofilm tensile strength resisting to erosion. *Water Sci. Technol.* 39 (7), 261–268.
- Rittmann, B.E., Stilwell, D., Garside, J.C., Amy, G.L., Spangenberg, C., Kalinsky, A., Akiyoshi, E., 2002. Treatment of a colored groundwater by ozone-biofiltration: pilot study and modeling interpretation. *Water Res.* 36 (13), 3387–3397.
- Sakoda, A., Wang, J., Suzuki, M., 1996. Microbial activity in biological activated carbon bed by pulse responses. *Water Sci. Technol.* 34 (5–6), 222–231.
- Wakao, N., Funazkri, T., 1978. Effect of fluid dispersion coefficients on particle-to-fluid mass transfer coefficients in packed beds. *Chem. Eng. Sci.* 33, 1375–1384.
- Walker, G.M., Weatherley, L.R., 1997. A simplified predictive model for biologically activated carbon fixed beds. *Process. Biochem.* 32 (4), 327–335.
- Wijeyekoon, S., Miho, T., Satoh, H., Matsuo, T., 2004. Effects of substrate loading rate on biofilm structure. *Water Res.* 38 (10), 2479–2488.
- Zhang, T.C., Bishop, P.L., 1994. Density, porosity and pore structure of biofilms. *Water Res.* 28 (10), 2267–2277.